Supporting Information

Van Vuuren *et al.* 10.1073/pnas.0711129105

STXT

SI Text

Overall Description of Methods. ***Emission scenarios.*** An emission database was compiled from recently published multigas stabilization scenarios. Most of these scenarios have been developed as part of the Stanford University-based Energy Modeling Forum (EMF) (1, 2) (for individual model description see below). Criteria for including scenarios here were coverage of relevant greenhouse gases (GHG) and radiatively important substances as well as publication in peer-reviewed literature. Not all integrated assessment models reported halocarbon in the detail required by the climate models. If that detail was not available, emissions were broken down by using the MiniCam results.

Harmonization. To allow a comparison, the emission scenarios were harmonized to common values for a base year. Emission values were set to the mean value of available emission inventories for the year 2000 by using gas-dependent scaling factors. These scaling factors were assumed to linearly converge to 1 in 2100 (see below).

Cost calculations. For cost calculations, we use a metric that can be computed for all these models, the net present value (NPV) of emission abatement cost; this is a proxy of the economic cost of an abatement policy allowing comparison across very different models. Abatement cost was defined as the abated emissions times the marginal price of carbon-equivalent emission reduction divided by 2.

$$\mathrm{NPV(AC)} = \int_{2010}^{2100} (1/(1+0.05)^{t-2000} * (E_{BL} - E_{Stab}) * P_{mar}/2)\,\mathrm{dt}$$

E_{BL} and E_{Stab}(emissions of the stabilization and baseline scenario) and P_{mar} (marginal price) are all calculated by the Integrated Assessment Model and vary over time.

Division by 2 is assumed to represent the fact that most reduction measures are not implemented at the marginal price but at much lower prices. In most cases, the relationship between emission reduction and the marginal price is a concave curve, which implies that a value >2 needs to be used. We have tested the relationship between the NPV calculated by the formula above and the NPV calculated on the basis of the real shape of the cost curve in IMAGE, MiniCam, and MESSAGE and found values ranging from slightly >2 up to 3–4, with higher values found for more stringent reduction targets. The value of 2, used here for simplicity (because the exact value is not known for the other models used here), leads thus to an overestimation of costs.

Climate modeling. The emission data have been used as input for the simple coupled gas-cycle climate model MAGICC and the Bern2.5CC intermediate-complexity climate–carbon cycle model. Extended model descriptions including references are given in *Model Descriptions: Climate and Integrated Assessment Models* below. Both models have been used in the IPCC Fourth Assessment Report (3). The reason to use these two models is to get a representation of the relevant uncertainties. The models are used here in their standard IPCC model setups.

Uncertainty ranges for the two climate models have been generated by considering impacts of climate sensitivity (CS)- and carbon cycle (CC)-related uncertainties individually and in combination (CS + CC). Ranges in MAGICC originate from 19 MAGICC runs emulating different coupled atmosphere/ocean general circulation models (AOGCMs) (mean ± 1 SD across 19 MAGICC runs, emulating different AOGCMS) The Bern2.5CC model ranges were obtained by combining different bounding assumptions regarding the behavior of the CO_2 fertilization effect, the response of heterotrophic respiration to temperature, and the turnover time of the ocean, thus approaching an upper bound of uncertainties in the carbon cycle. The effect of varying climate sensitivity from 1.5°C to 4.5°C has also been taken into account.

Harmonization of Emissions. We harmonize year-2000 emissions of the different scenarios to improve comparability. Various emission inventories of emissions for year 2000 are available, but it should be noted that emission estimates are affected by inevitable degrees of uncertainty. CO_2 emissions from energy and industrial sources are relatively well researched compared with other sources, but still, the most commonly used inventories for this source differ by ≈5% (see Table S1). ZST1

We used the mean of the available, most relevant inventories for our harmonization (Table S1). The differences among the ZST1 various inventories for emissions other than CO_2 are typically in the order of 10–15% of emissions. Interestingly, for most sources, the uncertainties in the base year emissions of the models used in this article are similar to the uncertainties in the estimates of the various inventories. In several cases, however, the mean of the inventories is different from the mean of the modeling results (CO_2, NO_x, CO).

Emissions of Halogenated Gases. The various halogenated gases have very different atmospheric lifetimes and radiative properties. Unfortunately, most models classify these gases using very different systems. For the calculations in the climate models, we used the classification as indicated in Table S1. Therefore, we ZST1 used a downscaling method to develop this information consisting of the steps below (directly available data were used instead for IMAGE and MiniCam): Emissions were first calculated for the emissions categories for which information was available, by using the normal harmonization procedure (categories of halogenated gases HFC, HFC23, PFC, and SF6).

These categories were then further broken down into the various gases by using the gas fractions in their respective aggregates of the MiniCam scenario.

Model Descriptions: Climate and Integrated Assessment Models. ***Climate models.*** *MAGICC.*

MAGICC is a simple coupled gas-cycle/climate model (4). MAGICC has been calibrated against a range of coupled atmosphere/ocean general circulation models (AOGCMs) and was used in the Intergovernmental Panel on Climate Change (IPCC) Third Assessment Report (TAR) and earlier IPCC reports to produce the standard projections of global-mean temperature and sea level change. In this study, MAGICC was run with calibration parameter sets to emulate output from 19 AOGCMs provided in the Program for Climate Model Diagnosis and Intercomparison (PCMDI) database (www-pcmdi.llnl.gov/) in preparation for the fourth IPCC Assessment report. The global carbon cycle response was adjusted to approximately emulate the lower-, medium-, and high-range CO_2 concentrations under the SRES A2 scenario [IPCC's Special Report on Emission Scenarios (5)] as provided by the World Climate Research Programme (WCRP) CMIP3 multimodel dataset of various carbon cycle models (6). Thus, for each emission scenario, 57 (equal to 19 × 3) runs were integrated with MAGICC. The means represent the averages across 19 AOGCM emula-

tions with medium carbon cycle settings. The ranges provided in the main text over climate and carbon cycle uncertainty are the means ± 1 SD for the subset of runs that assume high and low carbon cycle feedbacks.

Bern2.5CC. The Bern2.5CC reduced complexity climate model (7) includes components describing (*i*) the physical climate system, (*ii*) the cycling of carbon and related elements, and (*iii*), a module to calculate concentrations of non-CO_2 GHGs and radiative forcing by atmospheric CO_2, non-CO_2 GHGs, and aerosols (8, 9). The Bern2.5CC model is the latest of the Bern models used in all four IPCC Assessment Reports and in various IPCC technical papers and special reports.

The ocean physical component is the zonally averaged, three-basin circulation model of Stocker *et al.* (10), coupled to a zonally and vertically averaged atmospheric energy balance model (EBM), including an active hydrological cycle (11). The physical model setup and parameters are described in ref. 8. The ocean biogeochemical component is a simple description of the cycles of carbon, carbon isotopes, oxygen, and carbon-related tracers (12). Phosphate is taken as the biolimiting nutrient, and temporally and spatially constant stoichiometric ratios between biogenic fluxes were assumed. A prognostic description of export production was applied to account for changes in the ocean carbon cycle and atmospheric CO_2 driven by changes in ocean circulation (8).

The terrestrial biosphere component is the Lund–Pottsdam–Jena dynamic global vegetation model (LPJ-DGVM) at a 3.75 × 2.5° resolution as used by Joos *et al.* (9) and described in detail in refs. 13–15. The LPJ-DGVM is forced by Cramer/Leemans annual mean climatology plus interannual climate variability from the Hadley simulation (30-year recycled climate) plus changes in the fields of surface temperature, precipitation, and cloud cover. The cloud cover is calculated by means of scaling spatial patterns (9) with the global-mean surface temperature simulated by the EBM in response to projected radiative forcing. Land-use changes are not explicitly considered in the present simulations. Instead, carbon fluxes from land-use changes are prescribed externally in emission scenarios. The impact of climate change on terrestrial C-storage is included.

Finally, the module designed to calculate radiative forcing by atmospheric CO_2, non-CO_2 GHGs, and aerosols is based on work summarized in Fuglestvedt and Berntsen (16) and Joos *et al.* (9).

AQ: A

The different components of the Bern2.5CC climate-carbon cycle model have been tested and applied in a range of studies investigating past, present, and future carbon cycle behavior and its impact on climate (e.g., refs. 8, 9, 12, and 17–25). Results are broadly consistent with those from more comprehensive AOGCMs, coupled climate models, and observations.

AQ: B

The Bern2.5CC model ranges are based on the approach used in IPCC Third Assessment Report (9, 26): the low-CO_2 case was obtained by applying a fast mixing ocean and assuming heterotrophic respiration to be independent of global warming; the high-CO_2 case was obtained by applying a slow mixing ocean and capping CO_2 fertilization after the year 2000. Calculated anthropogenic emissions in the year 2000 for lower and upper bounds are 7.4 and 9.4 GtC/yr respectively, in accordance with the range of data-based estimates (27). Average ocean carbon uptake over the 1980–2000 period ranges between 1.91 and 2.53 GtC/yr, uptake from 1800 to 1995 is between 116.1 and 159.8 GtC and, thus, at the upper end of the current range of observational estimates (27). The effect of varying climate sensitivity from 1.5 to 4.5°C has been also taken into account. The model reference case is obtained with midrange behavior of the carbon cycle and a climate sensitivity of 3.2°C.

Integrated assesment models. *IMAGE.* IMAGE is an integrated assessment model for global change (28, 29). The main objectives of IMAGE are to contribute to scientific understanding and support decision-making by quantifying the relative importance of major processes and interactions in the society–biosphere–climate system. Two main components of the model are the description of the energy system and related emissions (the TIMER energy model) and land use and land cover and related emissions. The model versions used for this article (2.2 and 2.3) distinguish 17 world regions for socioeconomic modeling, whereas a 0.5 × 0.5 grid is used for many environmental parameters (30, 31). For climate change, the IMAGE model uses an adapted version of the MAGICC model in combination with methods for pattern scaling. In the context of climate-change policy scenarios, the IMAGE model is run in conjunction with the FAIR climate policy-analysis model (32). In this setup, IMAGE provides information on baseline emissions and mitigation options, whereas FAIR chooses the set of options that lead to lowest costs given a certain climate target and derived emission profile. The scenarios discussed in this article form a part of the studies published for looking into integrated reduction strategies (30, 31).

AIM. AIM is a generic name of the simulation models developed by the Asian Pacific Integrated Model team. The multiregion/multisector/multigas model AIM/CGE (Asia) was developed to analyze long-term stabilization scenarios. This model is a recursive dynamic computable general equilibrium (CGE) model based on a Global Trade Analysis Project energy–economy dataset (GTAP-EG) structure and programmed with GAMS/MPSGE. GTAP ver.5 database (base year = 1997) is used for the economic database and IEA energy statistics for the energy database. This is a long-term model with a time horizon from 1997 to 2100; it includes 18 world regions and 13 economic sectors (33). The AIM/CGE (Asia) is an update of the AIM/CGE (Energy) model (34) and includes a framework for both CO_2 and non-CO_2 gases. The model serves three sectors—production, household, and government—in each region. CO_2 and non-CO_2 gases are emitted by activities in each of these sectors.

IPAC. Integrated Policy Assessment model for China (IPAC) is a model framework developed by China's Energy Research Institute to analyze energy and emission-mitigation policies with focus on China (35). The IPAC framework is composed of several models including both bottom-up and top-down models, and model development has benefited from collaboration with other institutes. The IPAC-emission model, one of the main models in IPAC, is a revised version of the AIM/emission model developed by the National Institute for Environment Studies (NIES) (33). IPAC's energy sector's top-down module is based on the Edmonds–Reilly–Barns (ERB) model; it includes a partial equilibrium model focusing on the energy market but also an end-use module taken from the IPAC-AIM/technology model. This model provides a detailed energy demand analysis for China before 2030. For other regions, data are mostly used from the AIM, although other information has been added (National Communications, IEA, EIA, etc.). The land-use module was developed from the agriculture and land use (AgLU) model (36). The IPAC model works with nine regions: USA, Western Europe and Canada, Pacific Organisation for Economic Cooperation and Development (OECD), Eastern Europe and Former Soviet Union, China, South and East Asia, Middle East, Africa, and Central and South America. The model runs from 1990 to 2100. The time steps are in units of 5 years up to 2030, followed by time steps for 2050, 2075, and 2100.

AQ: C

AQ: D

EPPA. The Massachusetts Institute of Technology (MIT) Emissions Prediction and Policy Analysis (EPPA) model is a computable general equilibrium (CGE) model. Advantages of CGE models for analysis of environmental policy are their ability to capture the influence of a sector-specific (e.g., energy, fiscal, or agricultural) policy on other industry sectors, consumption, and international trade, and impacts on capital accumulation and

growth. The MIT EPPA model is a recursive-dynamic, 17-region CGE model of the world economy (37, 38), with considerable sectoral and energy technology detail, built on the economic and energy data from the GTAP dataset (39, 40) and additional data for the GHG (CO_2, CH4, N_2O, HFCs, PFCs and SF_6) and urban gas emissions (CO, VOC, NOX, SO_2, BC, OC, NH_4) recently updated to include the US EPA inventory data (41), and including endogenous costing of the abatement of non-CO_2 GHGs (42). It has been used extensively for the study of climate policy, climate interactions, and impacts and to study uncertainty in emissions and climate projections for climate models as discussed in greater detail in Paltsev *et al.* (38).

MiniCAM. The calculations presented here were conducted with the MiniCAM 2001 integrated assessment model (see refs. 43 and 44) for the equation structure). Its energy-economy roots can be traced back to Edmonds and Reilly (45). MiniCAM is a partial equilibrium energy–economic–agricultural model that also incorporates the set of climate and atmospheric models known as MAGICC (46, 47). The energy component of the MiniCAM solves world and regional energy supply and demand in 14 world regions from 1990 to 2095 using a 15-year time step. The MiniCAM begins with a representation of demographic and economic developments in each region and combines these with assumptions about technology development to describe an internally consistent representation of energy, agriculture, land-use, and economic developments that in turn shape global emissions and concentrations of GHGs. GHG concentrations in turn determine radiative forcing and climate change. The MiniCAM model focuses strongly on energy production, transformation, and use. The model tracks the production of fossil fuels, namely oil, natural gas, and coal as well as nonfossil primary energy forms including nuclear, wind, solar, and hydro. The model transforms primary energy forms to those that are consumed in final use. Transformation processes include refining, power generation, and hydrogen production. A variety of technology options are available to produce all of the end-use energy forms: liquids, gases, solids, electricity, and hydrogen. Electric generation technologies include fossil fuels (with or without geologic sequestration), biomass, and a number of non-carbon-emitting technologies (wind, solar PV, fusion, nuclear, hydroelectric, etc.). Energy is consumed in three final-use sectors: buildings, industry, and transportation. Emissions of a suite of aerosols and non-CO_2 GHGs are included, based on parameterization of emissions controls on local air pollutants (48–50). The version of the model used to produce the results in this work has now been replaced by an implementation using an object-oriented design paradigm (51).

MESSAGE. MESSAGE (Model for Energy Supply Strategy Alternatives and their General Environmental Impact) is a systems-engineering optimization model used for medium- to long-term energy system planning, energy policy analysis, and scenario development (52). The model provides a framework for representing an energy system with all its interdependencies from resource extraction, imports and exports, conversion, transport, and distribution to the provision of energy end-use services such as light, space conditioning, industrial production processes, and transportation. The model's current version, MESSAGE IV, provides information on the utilization of domestic resources, energy imports and exports, and trade-related monetary flows, investment requirements, the types of production or conversion technologies selected (technology substitution), pollutant emissions, interfuel substitution processes, and temporal trajectories for primary, secondary, final, and useful energy. MESSAGE is linked to the MACRO economic modeling framework (53, 54) which permits the estimation of internally consistent scenarios of energy prices and energy systems costs—derived from a detailed systems-engineering model (MESSAGE)—with economic-growth and energy-demand projections obtained from a macroeconomic model (MACRO). The framework operates at the level of 11 world regions. Integration of agriculture and forestry sectors in the MESSAGE–MACRO framework has been achieved through linkages to the land-use/climate policy dynamic integrated model of forestry and alternative land use (DIMA) model and the agriculture land use Agricultural Zones Model–Basic Linked System (AEZ–BLS) model. Although potentials for bioenergy supply and CO_2 mitigation via forest-sink enhancement are based on sensitivity analysis of the DIMA model, the AEZ–BLS framework provides important inputs with respect to agricultural drivers of GHG emissions, such as changes in rice cultivation, animal stock, and fertilizer use. In that sense, the MESSAGE–MACRO stands at the heart of the fully integrated IIASA assessment framework (55). Its principal results comprise the estimation of technologically specific multisector response strategies for alternative climate stabilization targets.

AQ: E

AQ: F

Correlation of Air Pollutants and Climate Policy. Fig. S1 shows the data of the various models for (*i*) emission reduction of fossil fuel CO_2 emissions in the mitigation scenarios compared with baseline emissions against (*ii*) the emissions reductions of air pollutants (SO_2, NO_x, VOC, and CO). ZSF1

For all air pollutants, emission reduction in mitigation scenarios were found to be correlated with CO_2 emission reductions as a result of climate policy-induced systemic changes in the energy system. For SO_2, this relationship even indicates that, on average, emission are reduced on par with CO_2. For the other three gases, emission reductions are smaller than those for CO_2, varying from ≈50% for NO_x to ≈30% for CO.

Key Model Outcomes Using Different Metrics. As indicated in the main text, different metrics are commonly used to describe outcomes of stabilization scenarios in the literature. Tables S2 and S3 summarize some key model outcomes of the MAGICC and Bern2.5CC models by using different common metrics. ZST2 ZST3

Comparison of MAGICC and Bern2.5CC Projections. The graphs in Figs. S2 and S3 compare the Bern2.5CC outcomes for projected CO_2 concentrations and temperature increase for each scenario in 2100 with those for the MAGICC model. The comparison leads to the following conclusions: Under default assumptions for the carbon cycle, the CO_2 concentrations found in MAGICC and Bern2.5CC are very similar. ZSF2,ZSF3

The variation in results for different carbon cycle assumptions is much larger in Bern2.5CC than in MAGICC, in particular on the high-concentration side.

In general, results show convergence between the two models on the low end of the concentration range.

Conclusions for projected radiative forcing from the two models (data not shown) are very similar to those for projected atmospheric CO_2 based on Fig. S2. This is not unexpected, because CO_2 dominates total anthropogenic radiative forcing. At the same time, however, radiative forcing is also impacted by gases other than CO_2. ZSF2

The comparison of projected temperature increase also lead to similar conclusions as those indicated for atmospheric CO_2 concentrations.

Comparison of Non-CO_2 Assumptions in the Two Climate Models. Fig. S4 shows model results for the projected temperature change in 2100 as compared with cumulative fossil and land use-related CO_2 emissions from 2000 to 2100. Best-fit lines for the BERN2.5CC and MAGICC models are shown. The results indicate that the 2100 temperature change does strongly depend on the 2000–2100 cumulative emissions (a linear fit results in high regression coefficients). The fit found for the Bern2.5CC model is slightly steeper than the one for MAGICC, The standard deviation of the residuals are 0.26°C and 0.29°C, respectively. ZSF4

1. van Vuuren DP, Weyant J, de la Chesnaye F (2006) Multigas scenarios to stabilise radiative forcing. *Energy Econ* 28:102–120.
2. Weyant JP, de la Chesnaye FC, Blanford GJ (2007) Overview of EMF21: Multigas mitigation and climate policy. *Energy Journal Special Issue* 3:1–32.
3. Solomon S, *et al.* (2007) *Climate Change 2007: The Physical Science Basis. Contribution of Working Group I to the Fourth Assessment* (Cambridge Univ Press, Cambridge, UK).
4. Wigley TML, Raper SCB (2001) Interpretation of high projections for global-mean warming. *Science* 293:451–454.
5. Nakicenovic N, *et al.* (2000) *Special Report on Emissions Scenarios* (Cambridge Univ Press, Cambridge, UK).
6. Friedlingstein P, *et al.* (2006) Climate-carbon cycle feedback analysis, results from the C4MIP model intercomparison. *J Clim* 19:3337–3353.
7. Plattner G-K, *et al.* (2008) Long-term climate commitments projected with climate–carbon cycle models. *J Clim* 21:2721–2751.
8. Plattner G-K, Joos F, Stocker TF, Marchal O (2001) Feedback mechanisms and sensitivities of ocean carbon uptake under global warming. *Tellus* 53B:564–592.
9. Joos F, *et al.* (2001) Global warming feedbacks on terrestrial carbon uptake under the Intergovernmental Panel on Climate Change (IPCC) emission scenarios. *Global Biogeochem Cycles* 15:891–907.
10. Stocker TF, Wright DG, Mysak LA (1992) A zonally averaged, coupled ocean-atmosphere model for paleoclimate studies. *J Clim* 5:773–797.
11. Schmittner A, Stocker TF (1999) The stability of the thermohaline circulation in global warming experiments., *J Clim* 12:1117–1133.
12. Marchal O, Stocker TF, Joos F (1998) A latitude-depth, circulation-biogeochemical ocean model for paleoclimate studies. Model development and sensitivities. *Tellus* 50B:290–316.
13. Cramer W (2001) Global response of terrestrial ecosystem structure and function to CO_2 and climate change: results from six global dynamic vegetation models. *Global Change Biol* 7:357–373.
14. Sitch S, *et al.* (2003) Evaluation of ecosystem dynamics, plant geography and terrestrial carbon cycling in the LPJ dynamic global vegetation model. *Global Change Biol* 9:161–185.
15. McGuire AD (2001) Carbon balance of the terrestrial biosphere in the Twentieth Century: Analyses of CO_2, climate and land-use effects with four process-based ecosystem models. *Global Biogeochem Cyc* 15:186–206.
16. Fuglestvedt J, Berntsen T (1999) A simple model for scenario studies of changes in global climate. *Working Paper 1999:2* (Center for International Climate and Environ Res, Oslo).
17. Stocker TF, Schmittner A (1997) Influence of CO_2 emission rates on the stability of the thermohaline circulation. *Nature* 388:862–865.
18. Marchal O, *et al.* (1999) Modelling the concentration of atmospheric CO_2 during the Younger Dryas climate event. *Clim Dyn* 15:341–354.
19. Joos F, Plattner G-K, Stocker TF, Marchal O, Schmittner A (1999) Global warming and marine carbon cycle feedbacks on future atmospheric CO_2. *Science* 284:464–467.
20. Plattner G-K, Joos F, Stocker TF (2002) Revision of the global carbon budget due to changing air-sea oxygen fluxes. *Global Biogeochem Cycle* 16.
21. Gerber S, *et al.* (2003) Constraining temperature variations over the last millennium by comparing simulated and observed atmospheric CO_2. *Clim Dyn* 20:281–299.
22. Gerber S, Joos F, Prentice IC (2004) Sensitivity of a dynamic global vegetation model to climate and atmospheric CO_2. *Global Change Biol* 10:1223–1239.
23. Joos F, Gerber S, Prentice IC, Otto-Bliesner BL, Valdes PJ (2004) Transient simulations of Holocene atmospheric carbon dioxide and terrestrial carbon since the Last Glacial Maximum. *Global Biogeochem Cycle* 18.
24. Koehler P, Joos F, Gerber S, Knutti R (2005) Simulated changes in vegetation distribution, land carbon storage, and atmospheric CO_2 in response to a collapse of the North Atlantic thermohaline circulation. *Clim Dyn* 25:689–708.
25. Orr JC (2005) Anthropogenic ocean acidification over the Twenty-first Century and its impact on marine calcifying organisms. *Nature* 437:681–686.
26. Prentice IC (2001) in *Climate Change 2001: The Scientific Basis. Contribution of Working Group I to the Third Assessment Report of the Intergovernmental Panel on Climate Change*, eds Houghton JT, *et al.* (Cambridge Univ Press, New York).
27. Manning AC, Keeling RF (2006) Global oceanic and land biotic carbon sinks from the Scripps atmospheric oxygen flask sampling network. *Tellus B* 58:95–116.
28. IMAGE-team (2001) *The IMAGE 2.2 Implementation of the SRES Scenarios. A Comprehensive Analysis of Emissions, Climate Change and Impacts in the 21st Century.* (Netherlands Environmental Asessment Agency, Bilthoven, The Netherlands).
29. MNP (2006) *Integrated Modelling of Global Environmental Change. An Overview of IMAGE 2.4* (Netherlands Environmental Asessment Agency, Bilthoven, The Netherlands).
30. van Vuuren DP, *et al.* (2007) Stabilizing greenhouse gas concentrations at low levels: An assessment of reduction strategies and costs. *Clim Change* 81:119–159.
31. van Vuuren DP, Eickhout B, Lucas P, den Elzen MGJ (2006) Long-term multi-gas scenarios to stabilise radiative forcing—Exploring costs and benefits within an integrated assessment framework. *Energy Journal Special Issue* 3:201–234.
32. den Elzen MGJ, Lucas P (2005) The FAIR model: A tool to analyse environmental and costs implications of climate regimes. *Environ Model Assessment* 10:115–134.
33. Fujino J, Nair R, Kainuma M, Masui T, Matsuoka Y (2006) Multi-gas mitigation analysis on stabilization scenarios using AIM global model *Energy Journal Special Issue* 3:343–353.
34. Kainuma M, Matsuoka Y, Morita T, Masui T, Takahashi K (2003) in *Climate Policy Assessment: Asia-Pacific Integrated Modeling*, eds Kainuma M, Matsuoka Y, Morita T (Springer, Tokyo).
35. Jiang K, Hu X, Songli Z (2006) Multi-gas mitigation analysis by IPAC *Energy Journal Special Issue* 3:425–440.
36. Sands RD, Leimbach M (2003) Modeling agriculture and land use in an integrated assessment framework. *Clim Change* 56:227.
37. Babiker M, *et al.* (2001) *The MIT Emissions Prediction and Policy Analysis (EPPA) Model: Revisions, Sensitivities, and Comparison of Results* (MIT Press, Cambridge, MA).
38. Paltsev S, *et al.* (2005) *The MIT Emissions Prediction and Policy Analysis (EPPA) Model: Version* 4 (MIT Joint Program for the Science and Policy of Global Change, Cambridge, MA).
39. Dimaranan B, McDougall R (2002) *Global Trade, Assistance, and Production: The GTAP 5 Data Base* (Center for Global Trade Analysis, Purdue Univ, West Lafayette, IN).
40. Hertel TW (1997) *Global Trade Analysis: Modeling and Applications* (Cambridge Univ Press, Cambridge, UK).
41. Mayer M, Hyman R, Harnisch J, Reilly J (2001) *Emissions Inventories and Time Trends for Greenhouse Gases and Other Pollutants* (MIT Press, Cambridge, MA).
42. Hyman RC, Reilly JM, Babiker MH, De Masin A, Jacoby HD (2002) Modeling non-CO2 greenhouse gas abatement. *Environ Model Assessment* 8:175–187.
43. Edmonds J, Clarke J, Dooley J, Kim SH, Smith SJ (2004) Stabilization of CO_2 in a B2 world: Insights on the roles of carbon capture and storage, hydrogen, and transportation technologies. *Energy Econ* 26:517–537.
44. Brenkert A, Smith SJ, Kim SH, Pitcher HM (2003) *Model Documentation: MiniCAM* 2001 (Pacific Northwest National Laboratory, Washington DC).
45. Edmonds J, Reilly J (1985) *Global Energy: Assessing the Future* (Oxford Univ Press, Oxford).
46. Wigley TML, Raper SCB (2002) Reasons for larger warming projections in the IPCC Third Assessment Report. *J Clim* 15:2945–2952.
47. Wigley TML, Raper SCB (1992) Implications for climate and sea-level of revised IPCC emissions scenarios. *Nature* 357:293–300.
48. Smith SJ (2005) Income and Pollutant Emissions in the ObjECTS MiniCAM Model. *J Environ Dev* 14:175–196.
49. Smith SJ, Pitcher H, Wigley TML (2005) Future sulfur dioxide emissions. *Clim Change* 73:267–318.
50. Smith SJ, Wigley TML (2006) Multi-gas forcing stabilization with the MiniCAM model. *Energy Journal Special Issue* 3:373–391.
51. Kim SH, Edmonds JA, Smith SJ, Wise M, Lurz J (2006) The Object-oriented Energy Climate Technology Systems (ObjECTS). Framework and Hybrid Modeling of Transportation. *Energy Journal Special Issue #4* 27:63–91.
52. Messner S, Strubegger M (1995) *User's Guide for MESSAGE III* (International Institute for Applied Systems Analysis, Laxenburg, Austria).
53. Manne A, Richels R (1992) *Buying Greenhouse Insurance: The Economic Costs of CO_2 Emissions Limits* (MIT Press, Cambridge, MA).
54. Messner S, Schrattenholzer L (2000) MESSAGE-MACRO: Linking an energy supply model with a macroeconomic model and solving it interactively. *Energy* 25:267–282.
55. Riahi K, Gruebler A, Nakicenovic N (2007) Scenarios of long-term socio-economic and environmental development under climate stabilization. *Forecast Soc Change* 74:887–935.

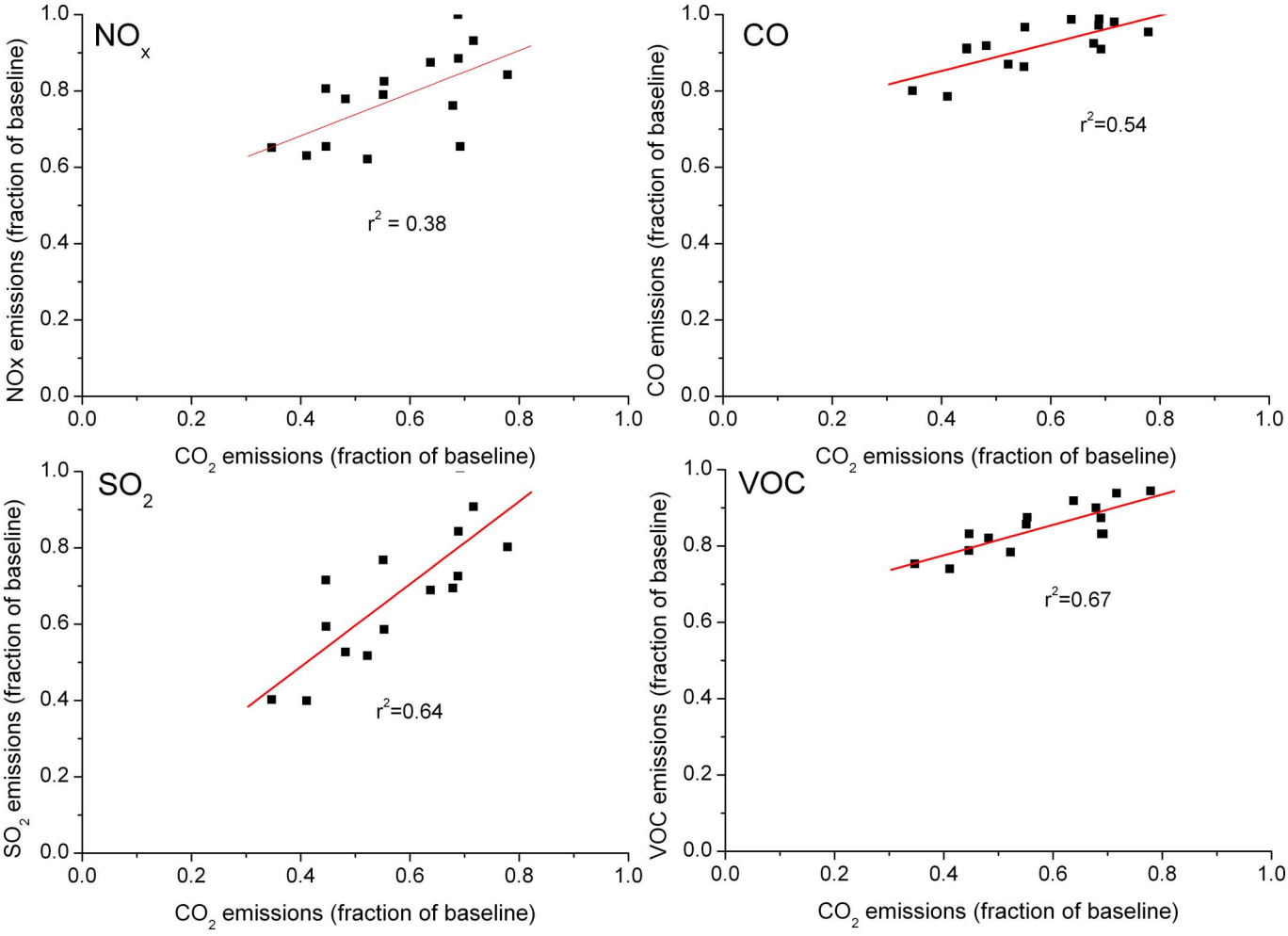

Fig. S1. Emission reductions for fossil fuel CO_2 emission versus emission reductions of air pollutants (NO_x, CO, SO_2 and VOC).

Sf1

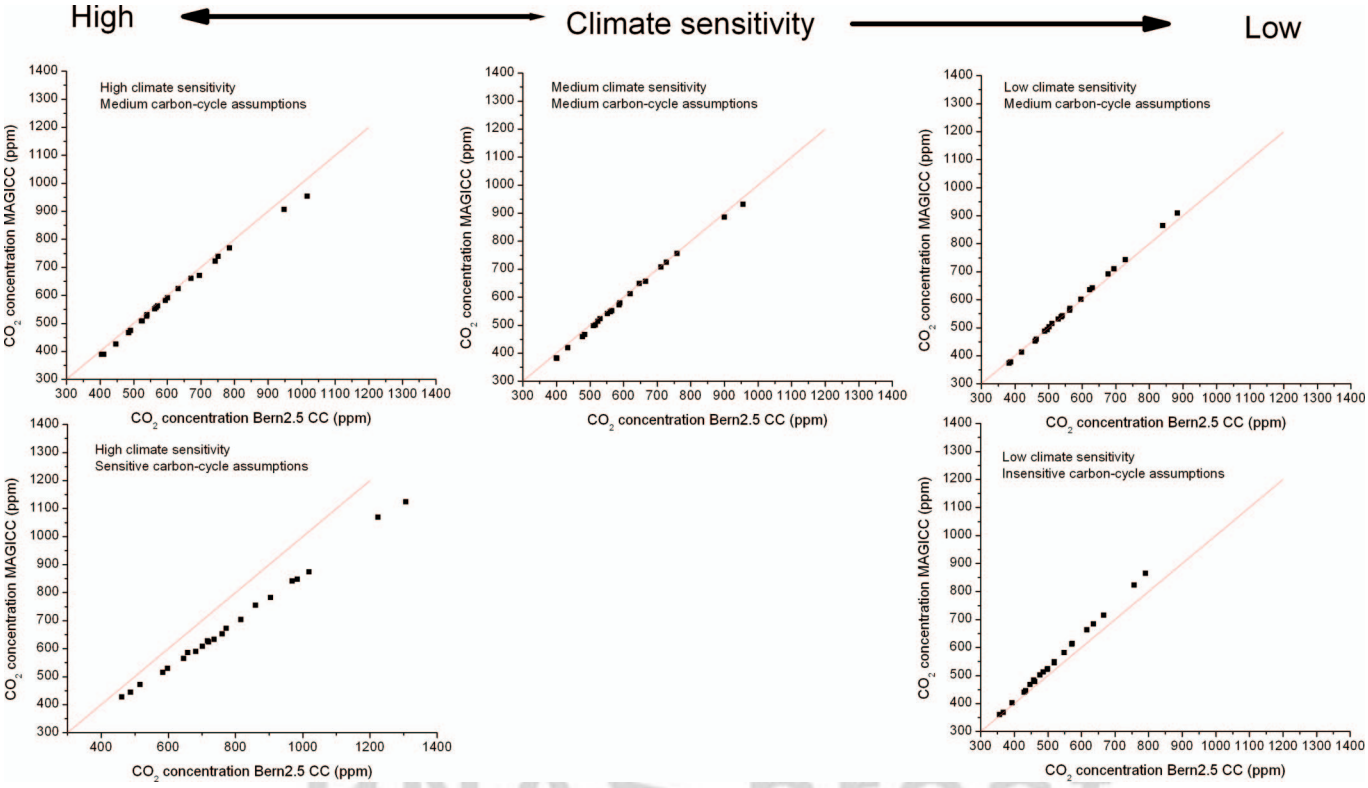

Fig. S2. Results for projected CO_2 concentrations from the Bern2.5CC model versus the MAGICC model. The graphs compare results under different combinations with respect to the climate sensitivity and carbon cycle assumptions. The low and high values for climate sensitivity and carbon cycle assumptions are defined per model as indicated in the model descriptions (see *Model Descriptions: Climate and Integrated Assessment Models* in *SI Text*).

Sf2

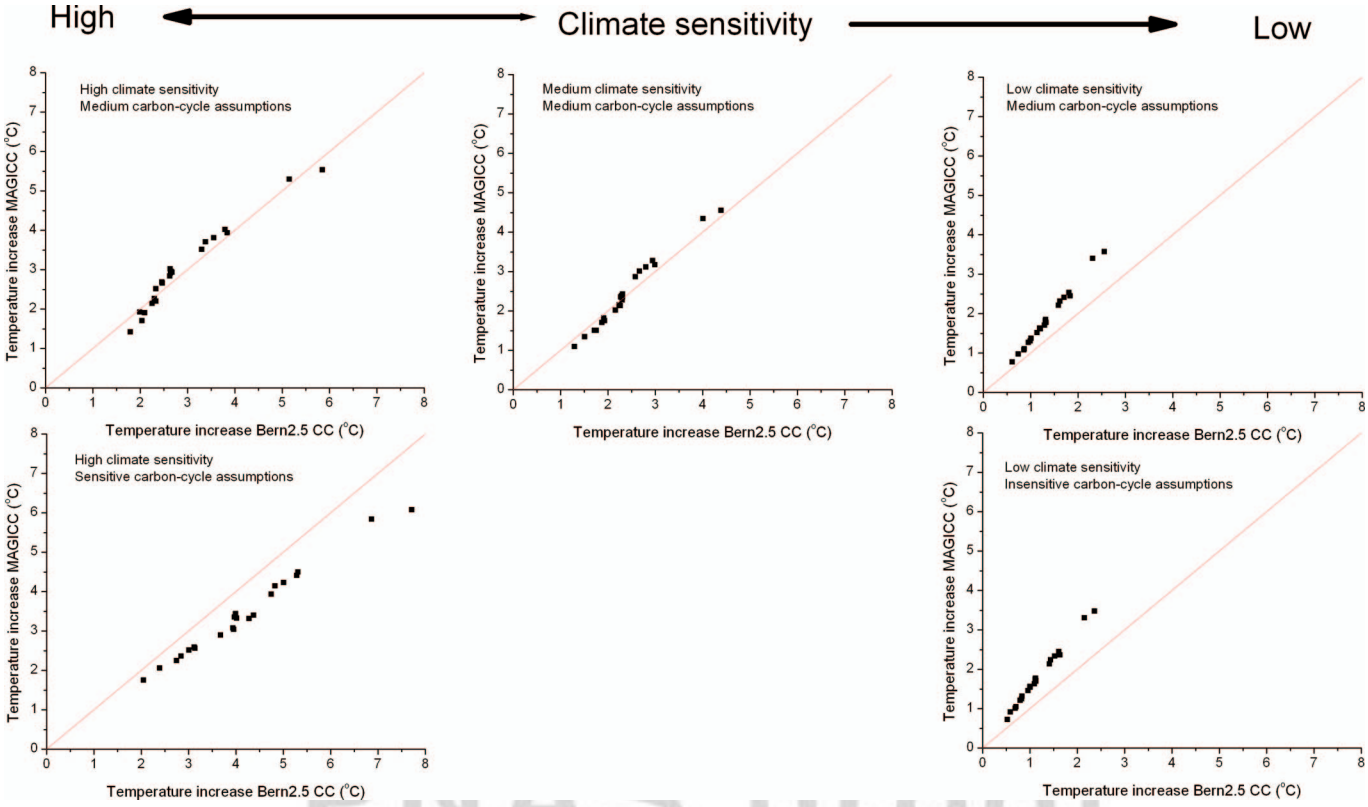

Fig. S3. Results for projected temperature increase for the Bern2.5CC model versus the MAGICC model. The graphs compare results under different combinations with respect to the climate sensitivity and carbon cycle assumptions. The low and high values for climate sensitivity and carbon cycle assumptions are defined per model as indicated in the model descriptions (see *Model Descriptions: Climate and Integrated Assessment Models* in *SI Text*).

Sf3

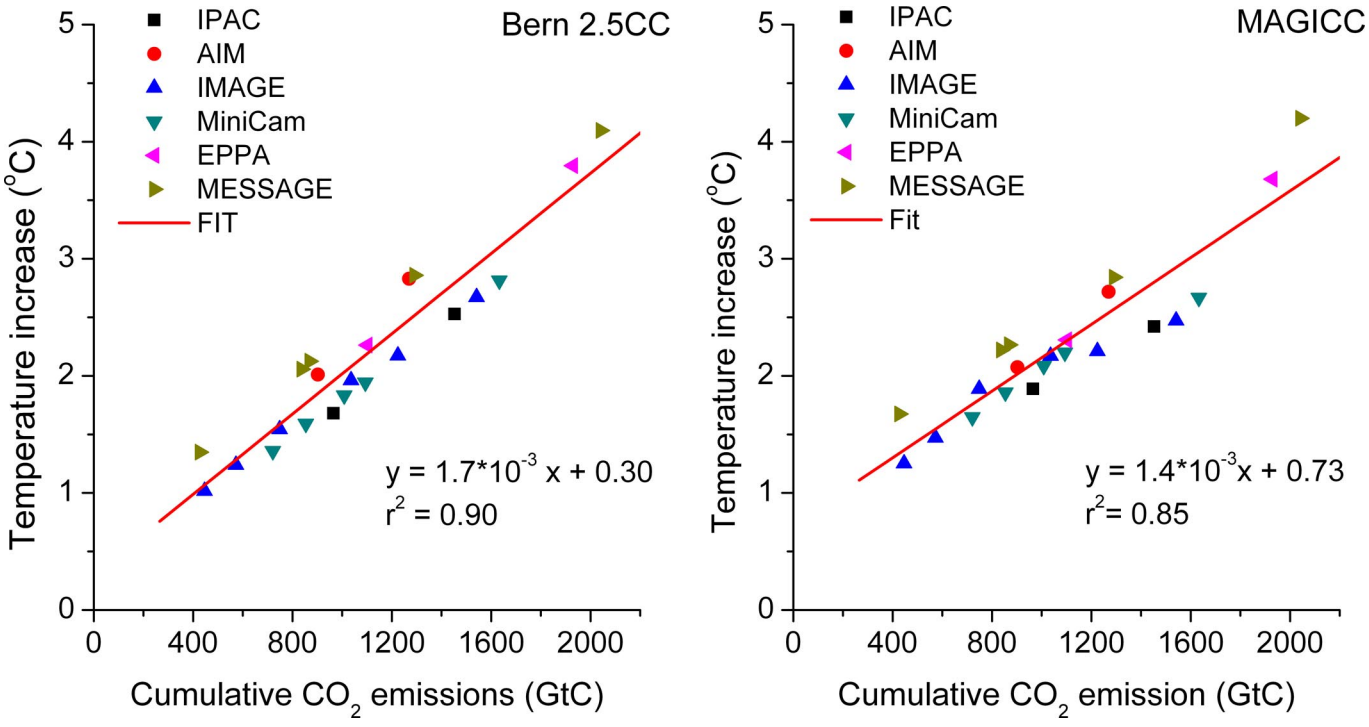

Fig. S4. Projected temperature increase vis-à-vis cumulative CO_2 emissions for the Bern2.5CC model (*Left*) and the MAGICC model (*Right*). The lines indicate the linear regression line for each set of results.

Sf4

Table S1. Historic emissions according to various emission inventories and emission values used for harmonization in this article

		EDGAR		EPA		Other		Values used for harmonization		Mean models	SRES	
Component	Unit	1990	2000	1990	2000	1990	2000	1990	2000	2000	1990	2000
Foss CO2	GtC	6.5	7.4			6.3 (1), 6.2 (2)	7.2 (1), 6.9 (2)	6.4	7.2	6.8	6.0	6.9
Defo CO2	GtC	0.5	0.7			2.2 (3)	2.1 (3)	1.1	1.1	1.1	1.1	1.1
Total CO2	GtC	7.0	8.2					7.5	8.3	7.9	7.1	8.0
CH4	MtCH4	302.0	321.0	275.7	278.8	366 (4)	326 (4)	288.8	299.9	297.8	309.7	322.9
N2O	Mt N2O-N	7.2	7.8	6.3	6.9			6.7	7.3	6.7	6.7	7.0
NOx	MtN	33.4	38.5			36.1 (4)	36/7 (4)	34.8	37.6	32.6	30.9	32.0
VOCs	Mt	153.2	186.3				250 (5)	153.2	186.3	174.8	139.1	141.4
CO	MtCO	846.0	1076.8			1098 (4)	1046 (4)	972.0	1061.4	898.4	879.0	877.1
SO2	MtS	74.6	79.1			65.7 (6), 70 (7)	54.1 (6) , 62 (7)	70.1	65.1	65.2	70.9	69.0
CF4		0.0105	0.0112	0.0138	0.0096	0.019 (8)	0.017 (8)	0.015	0.013		0.018	0.016
C2F6		0.0019	0.0026	0.0019	0.0027	0.001 (8)	0.001 (8)	0.002	0.002		0.001	0.002
HFC125		0.0000	0.0087			0.000 (8)	0.034 (8)	0.000	0.021		0.000	0.000
HFC134a		0.0000	0.0602			0.000 (8)	0.089 (8)	0.000	0.077		0.000	0.080
HFC143a		0.0000	0.0035			0.000 (8)	0.015 (8)	0.000	0.009		0.000	0.000
HFC227		0.0000	0.0404			0.000 (8)	0.000 (8)	0.000	0.020		0.000	0.000
HFC245		0.0000	0.0000			0.000 (8)	0.037 (8)	0.000	0.018		0.000	0.000
SF6		0.0047	0.0052			0.006 (8)	0.006 (8)	0.006	0.006		0.006	0.006
HFC23		0.0053	0.0067	0.0067	0.0083			0.006	0.007		0.000	0.000

Sources: EDGAR data was collected from the EDGAR website (www.mnp.nl/edgar). EPA data were collected from EPA (2006) *Global Anthropogenic Non-CO2 Greenhouse Gas Emissions: 1990–2020* (US Environmental Protection Agency, Washington, DC). SRES data were collected from Nakicenovic, *et al*. (2000) *Special Report on Emission Scenarios* (Cambridge Univ Press, Cambridge, UK). The data in the other columns are based on the following sources: (1) IEA (2005*) CO_2 Emissions from OECD and Non-OECD Countries* (Organisation for Economic Co-operation and Development , Paris); (2) CDIAC (2006) http://cdiac.esd.ornl.gov/trends/emis/em_cont.htm/; (3) Houghton RA (2003) Revised estimates of the annual net flux of carbon to the atmosphere from changes in land use and land management 1850–2000. *Tellus B* 55 378–390; (4) Cofala J, Amann M, Mechler R (2005) *Scenarios of World Anthropogenic Emissions of Air Pollutants and Methane up to 2030*, Technical report [International Institute for Applied Systems Analysis (IIASA), Laxenburg, Austria], available from: www.iiasa.ac.at/rains/global emiss/global emiss.html/; (5) Dentener F, *et al.* (2005). The impact of air pollutant and methane emission controls on tropospheric ozone and radiative forcing: CTM calculations for the period 1990–2030. *Atmos Chem Phys* 5:1731–1755; (6) Cofala, *et al.* see (4) above, but including EDGAR and Smith *et al*. for emissions not covered by Cofala; (7) Smith SJ, Pitcher H, Wigley TML (2005) Future sulfur dioxide emissions. *Clim Change* 73:267–318; (8) Smith SJ, Wigley TML (2006) Multi-gas forcing stabilization with the MiniCAM. *Energy Journal Special Issue* 3:373–391.

T1

Table S2. Key model outcomes MAGICC

		2100			Equilibrium	2100	
						Temperature, °C	
Model	Scenario	CO_2 concentration, ppm (range)	Radiative forcing, W/m^2 (range)	CO2-eq, ppm	Reported, W/m^2	1980–2000 (range)	Preindustrial
AIM	ref	648 (612–754)	6.1 (5.8–6.8)	872		2.9 (2.1–3.9)	3.4
	emf	523 (501–586)	4.0 (3.8–4.6)	593	4.5	1.8 (1.3–2.6)	2.4
IPAC	ref	707 (663–840)	6.7 (6.4–7.6)	980		3.3 (2.4–4.5)	3.8
	emf	541 (512–627)	4.9 (4.6–5.6)	696	4.5	2.4 (1.7–3.3)	2.9
IMAGE	ref	725 (683–847)	6.2 (5.9–7)	895		3.0 (2.2–4.1)	3.6
	emf	552 (524–633)	4.5 (4.2–5.2)	645	4.5	2.2 (1.6–3.1)	2.7
	53	612 (581–703)	5.0 (4.7–5.7)	710	5.3	2.4 (1.7–3.4)	2.9
	37	467 (445–529)	3.6 (3.4–4.2)	548	3.7	1.7 (1.2–2.5)	2.3
	29	420 (402–471)	2.8 (2.6–3.4)	475	2.6	1.3 (0.9–2.1)	1.9
	26	383 (368–427)	2.4 (2.2–2.9)	435	2	1.1 (0.7–1.8)	1.7
MiniCam	ref	756 (715–874)	6.5 (6.2–7.2)	935		3.1 (2.3–4.2)	3.7
	emf	572 (545–652)	4.4 (4.1–5.1)	636	4.5	2.1 (1.5–3)	2.7
	45	548 (521–623)	4.2 (3.9–4.8)	611	4.5	2.0 (1.5–2.9)	2.6
	40	501 (478–565)	3.7 (3.5–4.3)	557	4	1.8 (1.3–2.6)	2.3
	35	459 (440–515)	3.2 (3–3.8)	507	3.5	1.5 (1.1–2.2)	2.1
EPPA	ref	885 (823–1,068)	8.8 (8.4–9.7)	1438		4.3 (3.3–5.8)	4.9
	emf	580 (548–672)	4.9 (4.7–5.7)	703	4.5	2.4 (1.8–3.4)	3.0
MESSAGE	refa	931 (864–1,124)	9.3 (9–10.2)	1606		4.6 (3.5–6.1)	5.1
	emf	498 (468–589)	4.6 (4.3–5.4)	659	4.5	2.3 (1.6–3.3)	2.8
	refb	657 (614–781)	6.5 (6.2–7.4)	949		3.2 (2.4–4.4)	3.7
	46	514 (483–608)	4.7 (4.4–5.5)	672	4.5	2.4 (1.7–3.4)	2.9
	32	382 (361–444)	3.0 (2.7–3.7)	487	3.2	1.5 (1–2.4)	2.1

As reference year for preindustrial temperature, 1860 is used. Warming since preindustrial is approximated by adding 0.6°C to the 1980–2000 values.

T2

Table S3. Key model outcomes Bern2.5CC

		2100			Equilibrium	2100	
						Temperature, °C	
Model	Scenario	CO_2 concentration, ppm (range)	Radiative forcing, W/m² (range)	CO2-eq, ppm	Reported, W/m²	1980–2000 (range)	Preindustrial
AIM	ref	647 (571–860)	6.2 (5.5–7.7)	891		2.6 (1.4–4.7)	3.1
	emf	530 (477–658)	4.1 (3.5–5.3)	603	4.5	1.9 (0.8–3.1)	2.5
IPAC	ref	711 (616–968)	6.9 (6.1–8.6)	1016		2.9 (1.6–5.3)	3.5
	emf	552 (487–717)	5.1 (4.5–6.5)	731	4.5	2.3 (1.1–4.0)	2.9
IMAGE	ref	727 (636–984)	6.2 (5.5–7.8)	897		2.7 (1.4–4.8)	3.2
	emf	565 (499–736)	4.7 (4.0–6.1)	670	4.5	2.2 (1.0–3.9)	2.8
	53	620 (548–816)	5.1 (4.4–6.5)	722	5.3	2.3 (1.1–4.0)	2.8
	37	484 (434–597)	3.9 (3.3–5.0)	578	3.7	1.9 (0.8–3.0)	2.5
	29	434 (394–516)	3.1 (2.6–4.0)	499	2.6	1.5 (0.6–2.4)	2.1
	26	400 (368–462)	2.7 (2.2–3.4)	460	2	1.3 (0.5–2.0)	1.8
MiniCam	ref	759 (667–1,018)	6.6 (5.9–8.2)	963		2.8 (1.5–5.0)	3.3
	emf	586 (519–760)	4.7 (4.1–6.1)	675	4.5	2.3 (1.–3.9)	2.8
	45	561 (498–720)	4.5 (3.8–5.8)	647	4.5	2.2 (1.0–3.7)	2.7
	40	516 (461–645)	4.0 (3.4–5.2)	590	4	1.9 (0.8–3.1)	2.5
	35	478 (429–584)	3.5 (3.0–4.6)	542	3.5	1.7 (0.7–2.7)	2.3
EPPA	ref	899 (757–1,224)	9.0 (8.1–10.7)	1518		4.0 (2.1–6.9)	4.6
	emf	589 (519–773)	5.1 (4.4–6.6)	726	4.5	2.3 (1.1–4.0)	2.9
MESSAGE	refa	956 (791–1,307)	9.9 (8.9–11.6)	1785		4.4 (2.4–7.7)	4.9
	emf	510 (447–681)	4.9 (4.2–6.4)	699	4.5	2.3 (1.1–4.3)	2.8
	refb	665 (573–904)	7.0 (6.2–8.6)	1032		3.0 (1.6–5.3)	3.5
	46	524 (458–701)	5.0 (4.3–6.6)	711	4.5	2.3 (1.1–4.4)	2.8
	32	401 (356–488)	3.4 (2.7–4.4)	526	3.2	1.8 (0.7–2.8)	2.3

As reference year for preindustrial temperature, 1860 is used. Warming since preindustrial is approximated by adding 0.6°C to the 1980–2000 values.

T3